91-02475/

ICE FORCE MEASUREMENTS AT HONDO, ALBERTA
1983 - 1986

By

G. Van Der Vinne
Resource Technologies Department
Alberta Research Council

This report is a publication of the Alberta Co-operative Research Program in Transportation and Surface Water Engineering, participants of which are the Resource Technologies Department, Alberta Research Council; Alberta Environment; Alberta Transportation; and the Department of Civil Engineering, University of Alberta.

Edmonton, Alberta
Report No. SWE-88/05 March 1988

ABSTRACT

Ice forces can be an important component in the design of river engineering structures in Canada. In order to refine the ice force values given in Bridge design codes, a long term program was set up to measure ice forces on a bridge pier near Hondo, Alberta. This report is the last of a series of reports presenting the results of this program. The data from 1983 - 1986 are presented and compared with previous results. A general description of each year's ice run is given along with typical floe sizes, ice thicknesses, and ice forces. This data is used to estimate the compressive strength of ice for the various ice failure modes. The mode of failure - crushing, bending, splitting, or impact - determines the method of analysis.

The ice runs of 1983, 1985 and 1986 were found to be of average severity. No ice forces were measured in 1984. The 1983 ice run produced a maximum ice force of 0.52 MN when an ice floe with an estimated strength of 580 kPa failed by crushing. In 1985, an estimated strength of 960 kPa was obtained from a maximum crushing force of 0.86 MN. In 1986, a bending failure produced a maximum ice force greater than 0.43 MN and an estimated strength of at least 300 kPa. The 1-in-100 year compressive strength of ice is found to be approximately 1500 kPa when all 19 years of data are used in the analysis. The average positive air temperature before breakup was found to be inadequate as a meteorological index to predict ice strength.

ACKNOWLEDGMENTS

The work described in this report was made possible with funds provided by Alberta Transportation and the Resource Technologies Department, Alberta Research Council, under the auspices of the Alberta Co-operative Research Program in Transportation and Surface Water Engineering. Participants in this program are the Resource Technologies Department, Alberta Research Council; Alberta Environment; Alberta Transportation; and the Department of Civil Engineering, University of Alberta.

The data for this project was collected by W. Huiskamp, P. Mostert, T. Ridgway, J. Thompson and B. Trevor. The report was reviewed by D. Andres and R. Kornelson.

TABLE OF CONTENTS

		Page
Abstract		(i)
Acknowledgments		(ii)
Table of Contents		(iii)
List of Figures		(iv)
List of Tables		(v)
1.0	INTRODUCTION	1
2.0	FIELD INSTALLATION	3
3.0	RESULTS	4
	3.1 Ice Run Descriptions	4
	3.1.1 1983 Ice Run	4
	3.1.2 1984 Ice Run	6
	3.1.3 1985 Ice Run	6
	3.1.4 1986 Ice Run	7
	3.2 Ice Force Measurements	9
4.0	ANALYSIS	12
	4.1 Strength Calculations	12
	4.1.1 Crushing	12
	4.1.2 Bending	14
	4.1.3 Impact	15
	4.1.4 Splitting	19
	4.2 Statistical Variation of Annual Peak Events	20
	4.3 Ice Strength Prediction	20
5.0	SUMMARY AND RECOMMENDATIONS	25
6.0	REFERENCES	26

LIST OF FIGURES

		page
Figure 1	Location of instrumented pier near Hondo, Alberta	2
Figure 2	Cross section of Hondo bridge pier	3
Figure 3	Water level elevations at Hondo bridge pier, April 1983	5
Figure 4	Water level elevations at Hondo bridge pier, April 1986	8
Figure 5	Load histories from various failure types a) H85.04.12.00.02.05 (crushing) and H85.04.12.00.02.34 (bending)	11
	b) H85.04.11.23.58 14 (splitting) and H85.04.11.23.58.56 (impact)	11
Figure 6	Geometry of an impact event	16
Figure 7	Maximum annual ice force frequency distribution	22
Figure 8	Compressive ice strength frequency distribution	22
Figure 9	Comparison of the meteorological index with the compressive strength of ice at breakup	23

LIST OF TABLES

		page
Table 1	Peak forces and flow descriptions for various ice load events	10
Table 2	Compressive strengths calculated from crushing event data	13
Table 3	Compressive strengths calculated from bending event data	15
Table 4	Compressive strengths calculated from impact event data	18
Table 5	Compressive strengths calculated from splitting event data	19
Table 6	Maximum ice forces measured at Hondo, 1967-1986	21

1.0 INTRODUCTION

The forces exerted on bridge piers by ice during spring breakup are an important component in the design of these structures for cold regions. In the past, the Canadian Highway Bridge Design Code, which specified the application of an effective pressure of 2800 kPa based on the crushing strength of ice, was used for all design situations. This effective pressure was multiplied by the pier width and expected ice thickness to obtain a design force for a bridge pier. Concern was expressed that this force was too conservative at times and resulted in a costly over-design of piers.

Because information regarding the magnitude of these ice forces and strengths were lacking, a program to measure ice forces on bridge piers was set up in Alberta beginning in 1967. Each spring, ice forces and related data were measured at an instrumented bridge pier in the Athabasca River near Hondo, Alberta (figure 1). Two other sites were instrumented as well, one in the Pembina River near Pembridge and the other in Kneehills Creek, but data collection at both these sites had been discontinued before the time period covered by this particular report. Data recorded at these sites have been published in a number of previous reports: Neill, Saunders and Schultz (1971); Neill and Schultz (1972); Lipsett and Gerard (1980); and Huiskamp (1983).

This report presents an analysis of the data collected at Hondo from 1983 to 1986. The analysis includes the estimation of ice strengths from measured ice forces generated by various ice failure modes as well as a comparison of the magnitudes of these ice forces and strengths with those obtained in previous years at the same site. An attempt is also made to estimate ice strength using a simple temperature index.

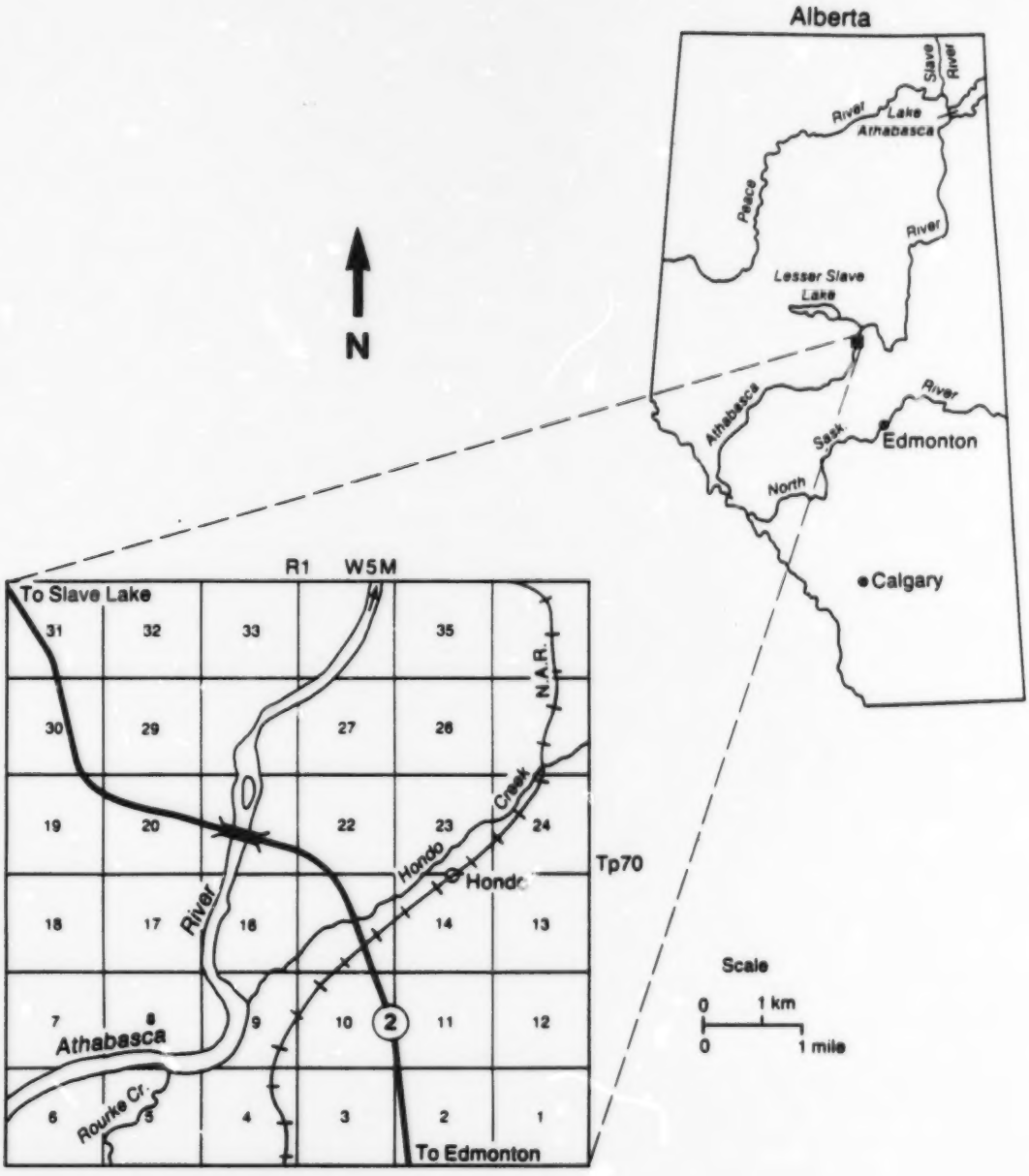

Figure 1 Location of instrumented pier near Hondo, Alberta

2.0 FIELD INSTALLATION

A load measurement system was installed in the nose section of pier 3 during the construction of the bridge over the Athabasca River near Hondo, Alberta. The longitudinal cross-section of this pier (figure 2) shows the configuration of the semicircular load beam and strain gauge load cell. The 2.32 m wide steel-encased, reinforced concrete load beam is pinned near the base of the pier and inclined 23° to the vertical. At the top of the beam, a load cell measures the reaction to ice forces. Two accelerometers, one longitudinal and one transverse, were mounted on the top on the pier to measure the corresponding pier vibrations. Data from the load cell and accelerometers were recorded both on strip charts and on FM tape. A water level recorder and float, housed in the stilling well in the center of the pier, monitored water levels throughout the ice run. A video camera mounted above the nose section provided a visual record of the ice load events.

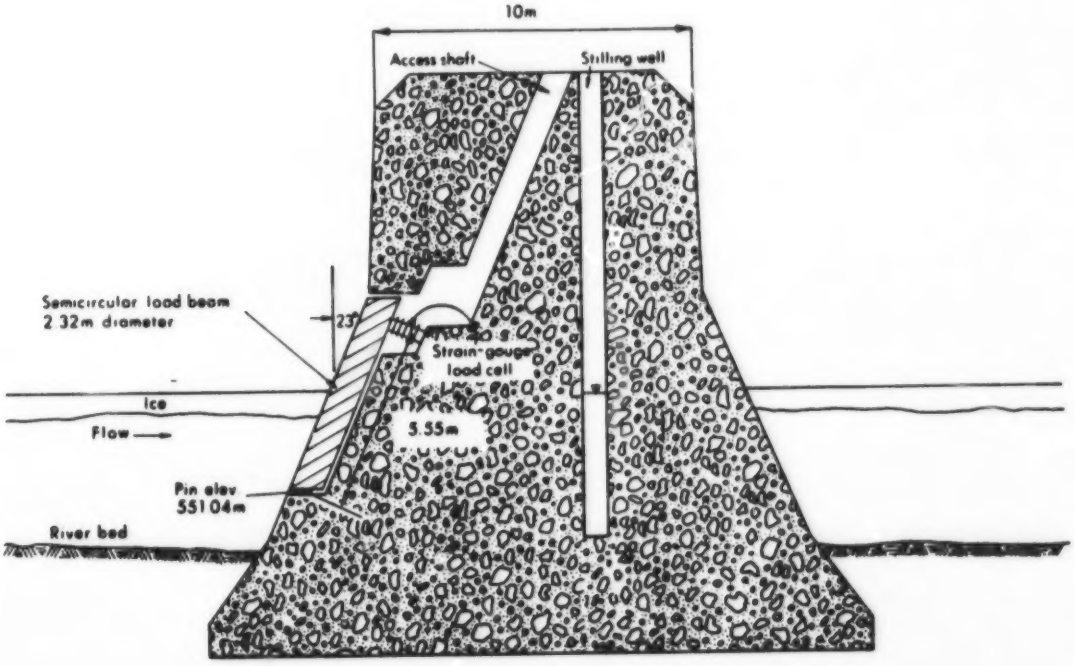

Figure 2 Cross section of Hondo bridge pier

3.0 RESULTS

Data collected for the ice force measurement program at Hondo from 1983 to 1986 are presented in this section. A general description of each year's ice run is given along with typical thicknesses, strengths, and forces. Ice forces measured using the load cell apparatus are also listed, along with related information such as ice failure modes, ice thicknesses, floe areas, and floe velocities.

3.1 Ice Run Descriptions

3.1.1 1983 Ice Run

Ice thickness measurements were taken on March 9 at various locations upstream of the bridge. The maximum observed thickness at this time was 1.25 m just downstream of the mouth of Rourke Creek (figure 1). Ice jamming has been observed at this location during ice formation in the fall (Lipsett and Gerard, 1980). The shoving of ice floes and the accumulation of frazil ice in the jam produces an ice cover which is thicker than average. Upstream of Rourke Creek, ice thicknesses ranged from 0.37 m to 0.44 m across the river width. Downstream of Rourke Creek, just upstream of Hondo Creek, the ice thickness varied between 0.65 m and 0.86 m. No ice strengths were measured.

Snowmelt occurred mostly between March 31 and April 5 according to the Twin Lakes snow pillow southwest of Barrhead (Alberta Environment, 1983), but the peak snow water equivalent was only 47 mm on March 31 so very little runoff was generated. In fact, the water level at the Hondo pier was falling before the first ice movement occurred at the bridge on April 17 (figure 3). This event was short-lived and only produced a small rise in water level. The main ice run occurred on April 19 and 20 and was accompanied by a 0.4 m rise in water level, as the surge moved past the bridge. The two smaller rises in water level which occurred on April 21 were also accompanied by the passage of ice.

The lack of significant runoff from snowmelt accompanied by a

relatively high average temperature, 4.8°C, during the melt period, produced a thermal breakup. That is, the ice had deteriorated significantly before breakup occurred and the stage increases associated with breakup were small. The ice floe thicknesses observed during breakup varied from 0.1 m to 0.45 m, much less than those measured on March 9. Ice forces were low as well. The maximum force measured during the ice run was 0.52 MN, produced when a 0.30 m thick floe failed by crushing against the pier. This is much less than the maximum observed force of 2.27 MN at Hondo in 1976 (Lipsett and Gerard, 1980).

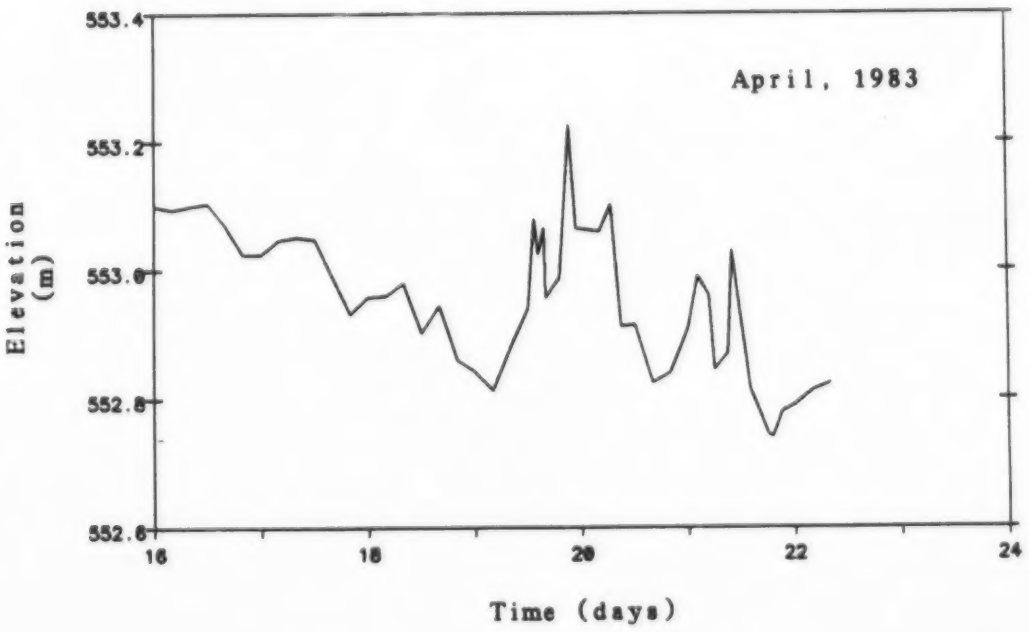

Figure 3 Water level elevations at Hondo bridge pier, April 1983

3.1.2 1984 Ice Run

Ice thicknesses and compressive strengths were measured upstream of the bridge on March 21 before significant melting had occurred. The maximum thickness, 1.13 m, was observed 0.5 km downstream of the mouth of Rourke Creek. The minimum observed thickness was 0.48 m. Horizontal compressive strengths ranged from 251 kPa to 3862 kPa with the average being about 2000 kPa.

No ice run occurred in 1984, because a lack of significant snow cover precluded the generation of sufficient runoff to break up the ice cover and produce an ice run. The peak snow water equivalent, measured at the Twin Lakes snow pillow, was only 51 mm and the main snow melt period occurred earlier than usual, between March 23 and April 2 (Alberta Environment, 1984). The runoff generated by this snowmelt was not sufficient to trigger breakup. Instead, the ice cover melted in place. The instrumentation was not set up to measure ice forces.

3.1.3 1985 Ice Run

Ice strengths and thicknesses were measured to establish pre-breakup conditions. Compressive strength tests performed in the field produced highly variable results. The average strength was approximately 1500 kPa but the individual values ranged from 261 kPa to 5010 kPa. Ice thicknesses varied between 0.9 m and 1.0 m.

Although positive daily mean temperatures were recorded as early as March 12 at Slave Lake and Athabasca, a period of negative daily mean temperatures occurred between March 21 and March 30 before significant snowmelt took place. Most of the snowmelt at the Twin Lakes snow pillow southwest of Barrhead occurred between April 2 and April 8 (Alberta Environment, 1985). The peak snow water equivalent for 1985, 104 mm, was twice that measured in either 1983 or 1984.

Significant movement of the ice cover at Hondo began on April 9, and the passage of ice continued intermittently until a jam formed on

April 12. The river was ice free at the bridge on April 9 when the instrumentation was set up, but that evening, ice sheets from the bend downstream of Hondo Creek moved by the bridge. The next evening, small sheets from around Hondo Creek started to run and on April 11, the jammed ice above Rourke Creek began to move downstream. This run continued until the next morning when a jam formed downstream of the bridge. The head of the jam was near Hondo Creek. No water level record is available because the water level recorder malfunctioned. The water surface elevation during the ice run was estimated to be approximately 554.6 m.

Although above average compressive strengths were observed at breakup, the ice forces were below average because the ice was thinner than usual. The largest recorded force, 0.86 MN, was produced by the crushing of an ice floe with a compressive strength of about 960 kPa and a thickness of 0.3 m.

3.1.4 1986 Ice Run

Compressive strength tests were performed in the field on March 11 to determine the ice strength prior to breakup. The strengths were found to be low compared to those of previous years. The average compressive strength was about 400 kPa, but the data ranged from 91 kPa to 1096 kPa. Ice thicknesses were also observed at this time. An ice thickness of 0.72 m was measured in the bend just upstream of the bridge and a thickness of 1.03 m was found near the mouth of Rourke Creek.

The main snowmelt, measured at the Twin Lakes snow pillow, occurred between March 27 and April 5 (Alberta Environment, 1986). The peak snow water equivalent at this site was 62 mm. The water level record at Hondo shows no evidence of a flood wave resulting from this snowmelt (figure 4). The water surface elevation slowly decreased with time. No large increases in water level occurred even when the ice went out.

The breakup at Hondo followed the same pattern as usual. The initial ice movement occurred on April 6, when the ice just upstream of

the bridge went out. On April 15, the ice from the first upstream bend came by the bridge in large sheets. On April 18, small sheets from the Hondo Creek area passed by the piers. The largest forces were measured during the run on April 19, when sheets as large as three-quarters of the river width square struck the pier. The reach upstream of the bridge was clear after this run, with only small ice debris moving past the bridge.

The largest ice forces were recorded on April 19, although the peak force is unknown because it occurred when the amplifiers were set for low range data. However, it is known that the peak was at least greater than 0.44 MN. In fact, the actual peak may be as much as double the value, judging from the shape of the trace on the strip chart during this load event. The average velocity of these large floes was 1.2 m/s but velocities as high as 1.7 m/s were observed. Ice thicknesses at breakup ranged between 0.1 m and 0.8 m.

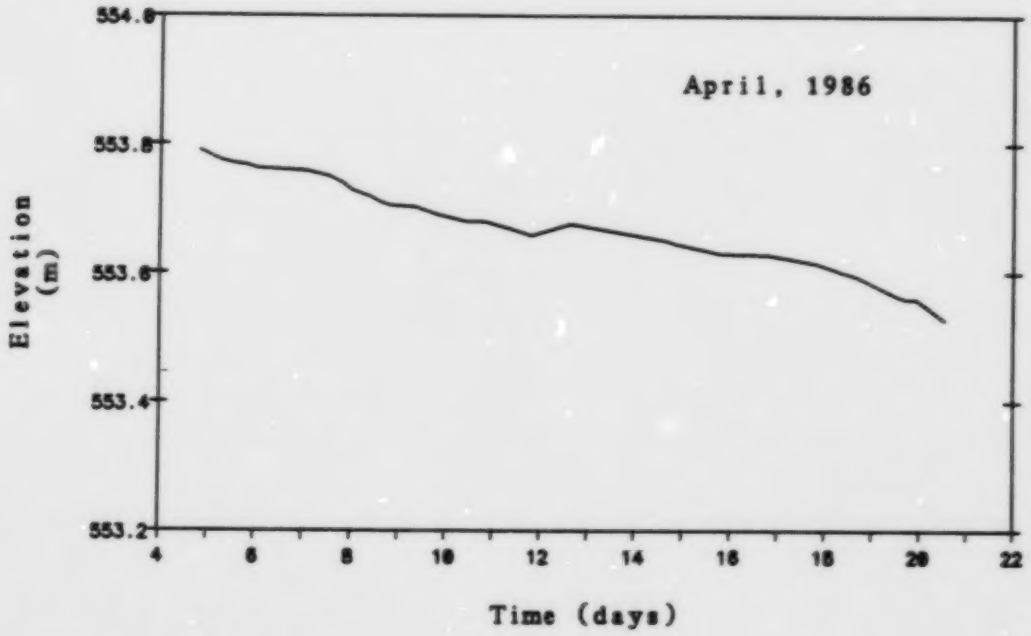

Figure 4 Water level elevations at Hondo bridge pier, April 1986

3.2 Ice Force Measurements

Ice forces were measured using the load cell apparatus installed in the Hondo pier. The maximum forces of selected ice load events recorded in 1983, 1985 and 1986 are listed in table 1. Floe characteristics, that is, thicknesses, areas and velocities are also included. Note that the time of the peak force identifies each event. For example, the label H83.04.18.12.58.24 designates a load event which occurred on April 18, 1983, at 12 hours, 58 minutes and 24 seconds.

The measured load events documented herein are the result of ice floes striking the bridge pier. Each load event has a characteristic shape which is determined by the failure mode of the ice floe. Some floes, such as the one producing the load sequence shown in figure 5 (a), for example, have more than one mode of failure. The first part of this load record exhibits high frequency fluctuations characteristic of crushing failures, while the second part of the record shows the lower frequency loading cycle produced when a floe repeatedly rides up the pier nose and fails by bending. Splitting failures and impact loads such as the ones shown in figure 5 (b), usually occur in smaller floes.

Table 1 Peak forces and flow descriptions for various ice load events

Event	Peak Force (MN)	Failure Mode	Ice Thickness (m)	Floe Area (m^2)	Floe Velocity (m/s)
H83.04.18.12.58.24	0.196	Bending	0.30		
13.02.29	0.239	Crushing	0.30		
13.10.29	0.208	Crushing	0.15		
13.11.07	0.343	Crushing	0.15		
13.26.46	0.262	Crushing	0.15		
13.27.06	0.444	Crushing	0.15		
13.34.47	0.516	Crushing	0.30	120	
H83.04.19.14.07.39	0.438	Crushing	0.30	4800	
15.25.50	0.388	Crushing	0.15		
20.01.19	0.459	Crushing	0.46		
20.01.47	0.447	Crushing	0.46		
H85.04.09.17.58.38	0.100	Impact	0.45	100	1.50
18.25.21	0.442	Crushing	0.60		1.50
H85.04.10.17.39.38	0.133	Impact	0.45	70	1.50
17.43.25	0.097	Impact	0.30	58	1.50
19.50.56	0.227	Impact	0.45	100	1.50
19.51.12	0.227	Crushing	0.30		1.50
H85.04.11.23.52.52	0.859	Crushing	0.30		1.50
23.53.50	0.778	Crushing	0.30		1.50
23.54.50	0.648	Crushing	0.30		1.50
23.56.32	0.448	Crushing	0.45		1.50
23.56.50	0.374	Impact	0.60	100	1.50
23.57.15	0.166	Impact	0.45	[illegible]	1.50
23.57.20	0.199	Impact	0.45	16	1.50
23.58.14	0.249	Splitting	0.45	93	1.50
23.58.56	0.365	Impact	0.45	100	1.50
H85.04.12.00.01.05	0.288	Splitting	0.20	9	1.50
00.02.05	0.748	Crushing	0.60		1.50
00.02.34	0.816	Bending	0.60		1.50
00.07.44	0.146	Impact	0.30	49	1.50
00.11.12	0.256	Impact	0.20	100	1.50
00.17.25	0.282	Impact	0.45	37	1.50
00.22.40	0.259	Crushing	0.30		1.50
00.23.20	0.405	Impact	0.30	100	1.50
00.26.00	0.391	Impact	0.60	49	1.50
H86.04.19.16.42.18	0.044	Crushing	0.15		1.23
16.47.40	0.077	Crushing	0.25		1.16
16.50.36	0.109	Crushing	0.30		1.04
16.51.19	0.103	Bending	0.30		0.69
16.54.36	0.100	Crushing	0.20		1.15
21.06.33	*0.436	Bending	0.77	16000	1.37
21.07.54	0.154	Crushing	0.20		0.99
21.08.48	0.281	Splitting	0.60	80	1.26
21.10.01	0.138	Crushing	0.10		1.33
21.11.05	0.397	Bending	0.50	900	1.41

*Peak force exceeded this value

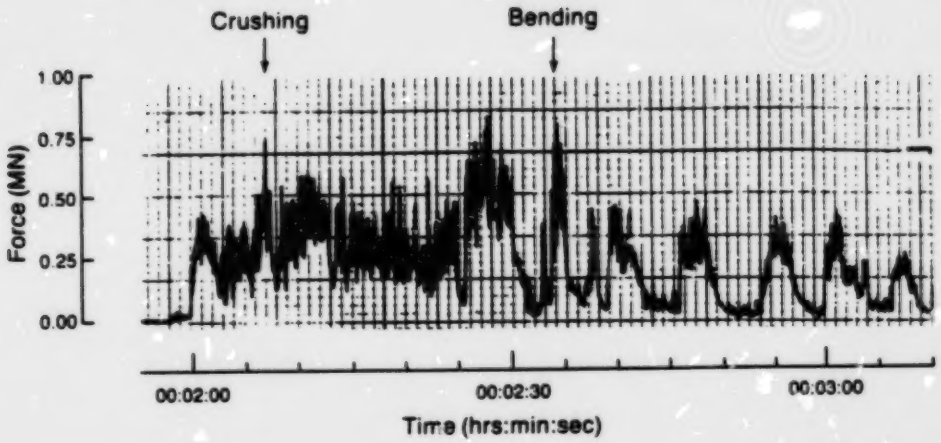

a) H85.04.12.00.02.05 (crushing) and
H85.04.12.00.02.34 (bending)

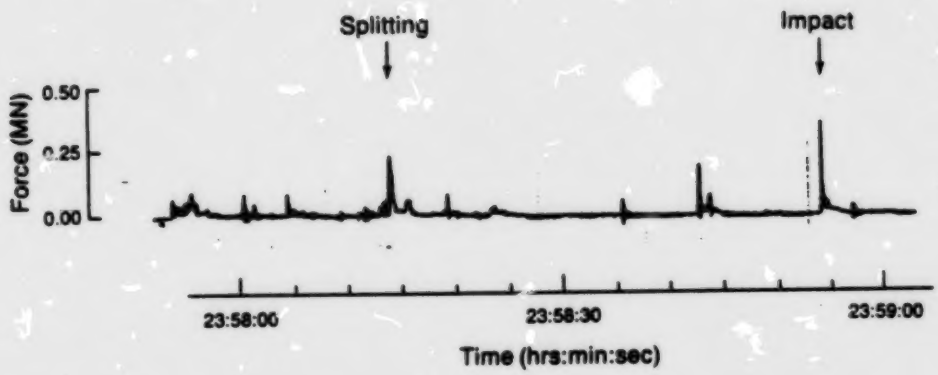

b) H85.04.11.23.58.14 (splitting) and
H85.04.11.23.58.56 (impact)

Figure 5 Load histories from various failure types

4.0 ANALYSIS

Ice load events are analyzed in two stages. First, ice strengths are determined for ice load events representing four different failure modes. Second, the yearly peak values of ice forces and strengths are compared with previous years' values to determine the probability of reoccurrence and the range of expected values.

4.1 Strength Calculations

Ice strengths, rather than ice forces, are specified in design codes so that a whole range of pier widths can be accommodated. In order to compare the force measurements from Hondo to current code specifications, the measured ice forces must be converted into ice strengths. The equations used to calculate ice strengths from ice forces depend on the mode of failure of the ice floes (Gerard, 1978). Lipsett and Gerard (1980) and Huiskamp (1983) present equations to analyze crushing, bending and splitting failures as well as impact events. These equations have been used in this analysis to obtain ice strengths associated with the various modes of failure.

4.1.1 Crushing

A crushing failure occurs when the nose of a pier is in contact with an ice floe across its full width. The equation used to calculate the ice force generated by this type of failure is:

$$[1] \quad F_c = k_c \sigma_c b h$$

where F_c is the ice force, k_c is the aspect ratio coefficient, σ_c is the compressive strength of ice, b is the width of the pier and h is the ice thickness.

The aspect ratio coefficient accounts for the difference between the compressive strength of ice and the effective pressure, which is

defined as the force divided by the area of contact, bh. Afanas'ev et al. (1971) developed the empirical relationship:

$$[2] \quad k_c = \sqrt{5(h/b)+1}$$

to determine the ratio between effective pressure and compressive strength.

Results of the analysis of crushing events using equations 1 and 2 are listed in table 2. The average compressive strength calculated for the 1986 data was 223 kPa, although values as high as 540 kPa were calculated. The average compressive strengths in 1983 and 1985 were approximately double that of 1986, 542 kPa and 585 kPa, respectively.

Table 2 Compressive strengths calculated from crushing event data

Event	Peak Force (MN)	Ice Thickness (m)	Effective Pressure (kPa)	Aspect Ratio Coefficient	Compressive Strength (kPa)
H83.04.18.13.02.29	0.239	0.30	343	1.283	268
13.10.06	0.208	0.15	598	1.150	520
13.11.07	0.343	0.15	986	1.150	857
13.26.46	0.262	0.15	753	1.150	654
13.27.06	0.444	0.15	1276	1.150	1109
13.34.47	0.516	0.30	741	1.283	578
H83.04.19.14.07.39	0.438	0.30	629	1.283	490
15.25.50	0.388	0.15	1115	1.150	969
20.01.19	0.459	0.46	430	1.411	305
20.01.47	0.447	0.46	419	1.411	297
18.25.21	0.442	0.60	318	1.514	210
19.51.12	0.227	0.30	326	1.283	254
H85.04.11.23.52.52	0.859	0.30	1234	1.283	962
23.52.50	0.778	0.30	1118	1.283	871
23.54.50	0.648	0.30	931	1.283	726
23.56.32	0.446	0.45	429	1.404	306
00.02.05	0.748	0.60	537	1.514	355
00.22.40	0.259	0.30	372	1.283	290
H86.04.19.16.42.18	0.044	0.15	126	1.150	110
16.47.40	0.077	0.25	133	1.240	107
16.50.36	0.109	0.30	157	1.283	122
16.54.36	0.100	0.20	216	1.196	180
21.07.54	0.154	0.20	332	1.196	277
21.10.01	0.138	0.10	595	1.103	540

The highest calculated strength was 1109 kPa in 1983, while in 1985, it was 962 kPa. These compressive strengths were considerably lower than those obtained from core samples before breakup.

4.1.2 Bending

If an ice floe fails in flexure before crushing develops over the full pier width, it is classified as a bending failure. This mode of failure only occurs on inclined pier noses such as the Hondo pier nose. It is characterized by a large ice floe riding up the pier nose and then breaking into two or three wedges.

The maximum horizontal force, F_B, generated by this failure can be calculated using the equation developed by Frederking (1980) and modified by Lipsett and Gerard (1980):

$$[3] \quad F_B = k_B C_\delta \sigma_t h^2$$

where C_δ is the coefficient for the number of wedges, σ_t is the tensile strength of ice and k_B is defined as:

$$[4] \quad k_B = [(1.16+0.0325\xi)+(2.26+0.0825\xi)a/l]\xi/3$$

where a is the truncation distance of the wedge approximated by the radius of the pier nose, l is the characteristic length of the ice given by

$$[5] \quad l = 15.56\, h^{3/4}$$

and ξ is the ratio of horizontal to vertical forces determined from the nose angle from horizontal, α, and the friction angle, ϕ, and is given by:

$$[6] \quad \xi = \tan(\alpha+\phi)$$

The value for C_δ can be determined from:

$$[7] \quad C_\delta = \tan \delta/2 \sum_{n=1}^{N} \sin[\delta/2+(n-1)\delta]$$

where n is the number of wedges formed and δ is the angle between the two edges of the wedge.

To analyze the bending events listed in table 3, C_δ was taken to be 1.284, the average of the values for two and three wedges, and the force ratio was found to be 4.33 for a nose angle of 67° and an assumed friction angle of 10°. For breakup conditions, the ice temperature is about 0°, so the compressive strength can be taken as 1.18 times the tensile strength (Lipsett and Gerard, 1980). The compressive strengths calculated using the above values are similar to the compressive strengths calculated for the crushing events listed in table 2.

4.1.3 Impact

An impact event occurs when an ice floe does not have sufficient kinetic energy to develop crushing over the full width of the pier. The ice strength can be found using the principle of conservation of energy, that is, the work done to stop the floe is equal to the original kinetic energy of the floe (Lipsett and Gerard, 1980) and:

$$[8] \quad \int_0^X F(x)\, dx = mV^2/2$$

Table 3 Compressive strengths calculated from bending event data

Event	Peak Force (MN)	Ice Thickness (m)	Tensile Strength (kPa)	Comprehensive Strength (kPa)
H83.04.18.12.58.24	0.196	0.30	659	777
H85.04.12.00.02.34	0.816	0.60	770	908
H86.04.19.16.51.19	0.103	0.30	346	408
21.06.33	*0.436	0.77	258	304
21.11.05	0.397	0.50	525	620

*Peak force exceeded this value

where m is the mass of the ice floe, V is the velocity, F(x) is the force at any depth, x, and X is the maximum penetration depth. Ice strength can be substituted into equation 8 using equation 1 if the contact area, y, is used rather than the pier width, b. For a circular pier nose such as the Hondo pier nose, x, y and k_c can be written as functions of the angle, β (Huiskamp, 1983), such that

$$[9] \quad x = R\,(1 - \cos\beta)$$

$$[10] \quad y = 2 \cdot R \sin\beta$$

and

$$[11] \quad k_c = \sqrt{2.5h/(R \cdot \sin\beta) + 1}$$

where R is the radius of the pier nose (figure 6).

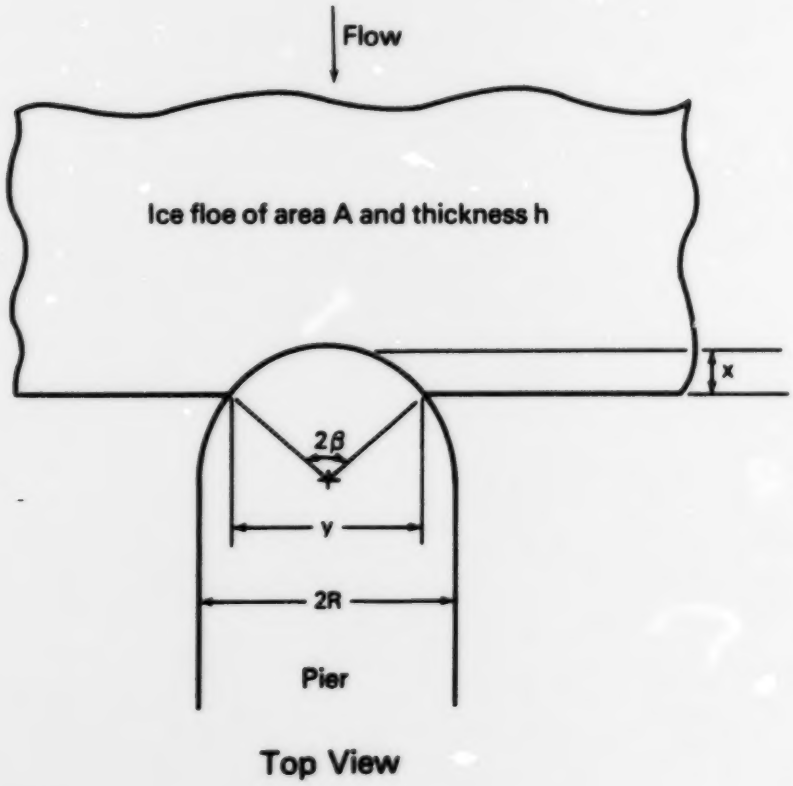

Figure 6 Geometry of an impact event

Together, these functions can be solved numerically to provide both ice strengths and penetration depths if the maximum ice force is known (Huiskamp, 1983). The results of this analysis are listed in table 4. Only events from 1985 were analyzed; impact events from other years could not be analyzed because critical floe information was not available.

The calculated penetration depths were compared with available measured penetration depths to check the validity of this analysis. In many cases, ice debris accumulating at the contact point obscured the view of the penetration depth making measurement impossible. Even when the view was clear, the measurement was only accurate to the first decimal place. The differences between the observed penetration depths and the corresponding calculated values is not large, considering the accuracy of the data. For example, event H85.04.12.00.07.44 had an observed penetration depth of 0.2 m while the calculated value was 0.14 m (table 4). This is within the accuracy of the data. In cases such as event H85.04.09.17.58.38, the observed penetration depth is less than the calculated value because the analysis assumed that the floe came to a complete stop when, in fact, it rotated off the pier before stopping. The observed value should not be larger than the calculated value, as it is in event H85.04.11.23.56.50, unless the ice strength is not consistent throughout the floe. The edge of the floe may have been weaker, causing the pier to penetrate more easily.

The average compressive strength obtained from this analysis, 363 kPa, is less than that obtained from either the crushing or bending analyses. This may be because larger floes with low strengths are more likely to break into smaller floes during the course of an ice run and it is these smaller floes which produce the impact events. Still, the highest strength obtained from the impact analysis, 921 kPa, is comparable to the highest strengths obtained from the crushing and bending analyses, so some of the stronger floes must break apart as well.

Table 4 Compressive strengths calculated from impact event data

Event	Peak Force (MN)	Ice Thickness (m)	Floe Area (m^2)	Floe Velocity (m/s)	Observed Penetration (m)	Calculated Penetration (m)	Compressive Strength (kPa)
H85.04.09.17.58.38	0.100	0.45	100	1.5	0.4	0.58	76
H85.04.10.17.39.38	0.133	0.45	70	1.5		0.32	120
17.43.25	0.097	0.30	58	1.5		0.25	158
19.50.36	0.227	0.45	100	1.5	0.3	0.28	201
H85.04.11.23.56.50	0.374	0.60	100	1.5	0.4	0.21	258
23.57.15	0.166	0.45	8	1.5		0.03	310
23.57.20	0.199	0.45	16	1.5		0.05	319
23.58.56	0.365	0.45	100	1.5		0.17	400
H85.04.12.00.07.44	0.146	0.30	49	1.5	0.2	0.14	289
00.11.12	0.256	0.20	100	1.5		0.11	921
00.17.25	0.282	0.45	37	1.5		0.08	389
00.23.20	0.405	0.30	100	1.5		0.10	888
00.26.00	0.391	0.60	49	1.5		0.10	388

4.1.4 Splitting

In some cases, a splitting failure occurred before a peak load could be developed from another failure mode. In previous reports (Lipsett and Gerard, 1980 and Huiskamp, 1983), it was noted that splitting failures occurred in an ice sheet after a series of bending failures. That is, once the ice sheet was small enough, a splitting failure occurred rather than another bending failure. If a splitting failure was analyzed as a bending event, a lower bound on ice strength could be obtained for the event. A lower bound on ice strength could also be estimated by performing an impact analysis because it was noted that some splitting failures occurred in smaller floes where impact loads were likely to occur.

Both bending and impact analysis were carried out on the three bending events listed in table 5. The ice strengths obtained from these two analyses were comparable except for the high strengths found in event H85.04.12.00.01.05. In this latter event the impact strength estimate may not be accurate because only a very small aspect ratio, y/h=0.04, was generated before failure occurred. The validity of using equation 2 in this range of aspect ratio has not been confirmed so it may be better to use only the bending strength in this case.

Table 5 Compressive strengths calculated from splitting event data

Event	Peak Force (MN)	Ice Thickness (m)	Floe Area (m^2)	Floe Velocity (m/s)	Compressive Strength (Bending) (kPa)	Compressive Strength (Impact) (kPa)
H85.04.11.23.58.14	0.249	0.45	100	1.50	261	251
H85.04.12.00.01.05	0.288	0.20	9	1.50	1528	2446
H86.04.19.21.08.48	0.281	0.60	80	1.26	166	212

4.2 Statistical Variation of Annual Peak Events

The maximum recorded forces at Hondo for each year of record are listed in table 6 along with their associated thicknesses and strengths. The relative severity of these events can be shown by developing probability plots of the data. Probability plots of maximum ice forces and ice strengths are shown in figures 7 and 8. The Weibull formula was used to determine the plotting positions for the data. Both the maximum ice forces and the associated strengths can be approximated by a normal distribution. The 1983 to 1986 maximum ice forces are all somewhat less than average, yet the ice strengths are in the mid-range. Variations in ice thickness account for this difference. This additional data does not change the distribution significantly; the 1-in-100 year ice strength is slightly less than 1500 kPa, while Huiskamp (1983) found it to be approximately 1400 kPa.

4.3 Ice Strength Prediction

Lipsett and Gerard (1980) used a simple meteorological index as a first attempt to estimate the ice strength at breakup. They used the average positive mean daily temperature before breakup to define the meteorological conditions leading up to the ice run. The mean daily temperatures recorded at Slave Lake and Athabasca were averaged to establish the temperatures at Hondo. Figure 9 shows this index plotted against the compressive strength of the ice at breakup. The data from 1983 to 1986 has been added to the previous data from Lipsett and Gerard (1980) and Huiskamp (1983). The dashed line indicates a general trend of increased compressive strength with increased meteorological index, but there is considerable scatter. A high index would result in a relatively quick snowmelt which would lead to a rapid rise in water level and possibly produce mechanical breakup if there was sufficient snow cover to begin with. A high compressive strength also indicates mechanical breakup because breakup occurs before the ice strength has deteriorated significantly. A low compressive strength on the other hand, indicates a thermal breakup where the ice was largely deteriorated in place before the ice run occurred.

Table 6 Maximum ice forces measured at Hondo, 1967-1986

Year	Thickness (m)	Force (MN)	Strength (kPa)	Failure Mode	Thaw Index
1967	0.50	0.64	383	Crushing	2.15
1968	0.30	0.20	224	Crushing	1.12
1969	0.84	1.65	1018	Bending	5.26
1970	0.60	0.91	432	Crushing	1.92
1971	0.84	1.20	740	Bending	
1972	0.84	1.80	1109	Bending	1.26
1973	0.50	0.40	239	Crushing	1.30
1974	0.91	1.44	764	Bending	3.19
1975	0.91	1.47	781	Bending	3.00
1976	1.00	2.27	1200	Splitting	6.85
1977	0.84	1.60	990	Bending	6.22
1978	0.30	0.30	336	Crushing	1.38
1979	0.70	1.07	417	Crushing	2.00
1980	1.60	1.08	192	Bending	4.00
1981	0.50	0.15	250	Bending	2.25
1982	1.20	1.44	449	Bending	3.19
1983	0.30	0.52	578	Crushing	4.82
1985	0.30	0.86	962	Crushing	2.94
1986	0.77	*0.44	304	Bending	0.80

*Peak forces exceeded this value

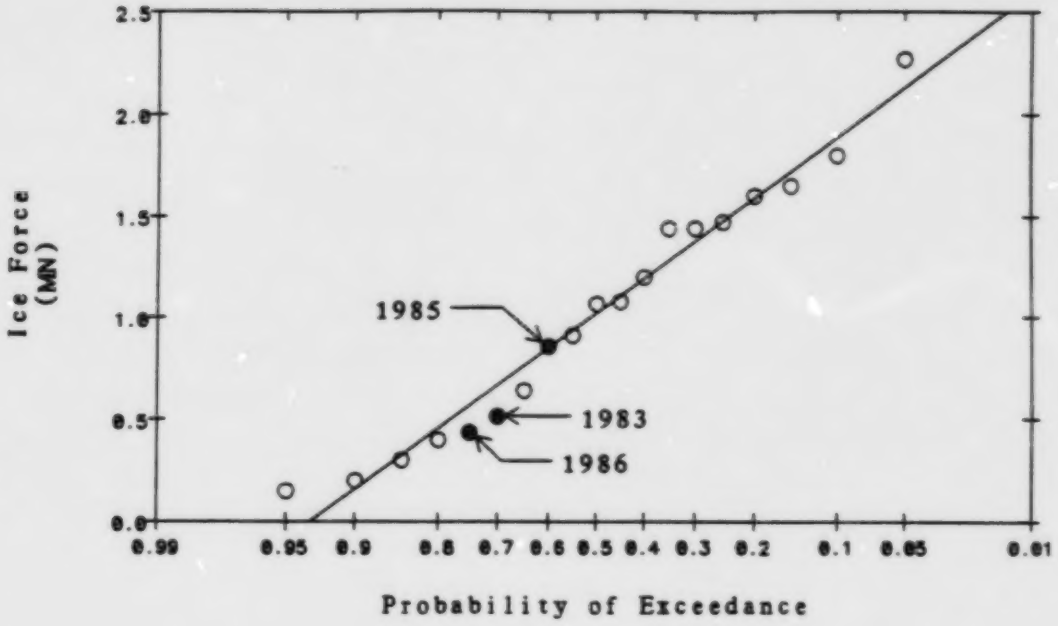

Figure 7 Maximum annual ice force frequency distribution

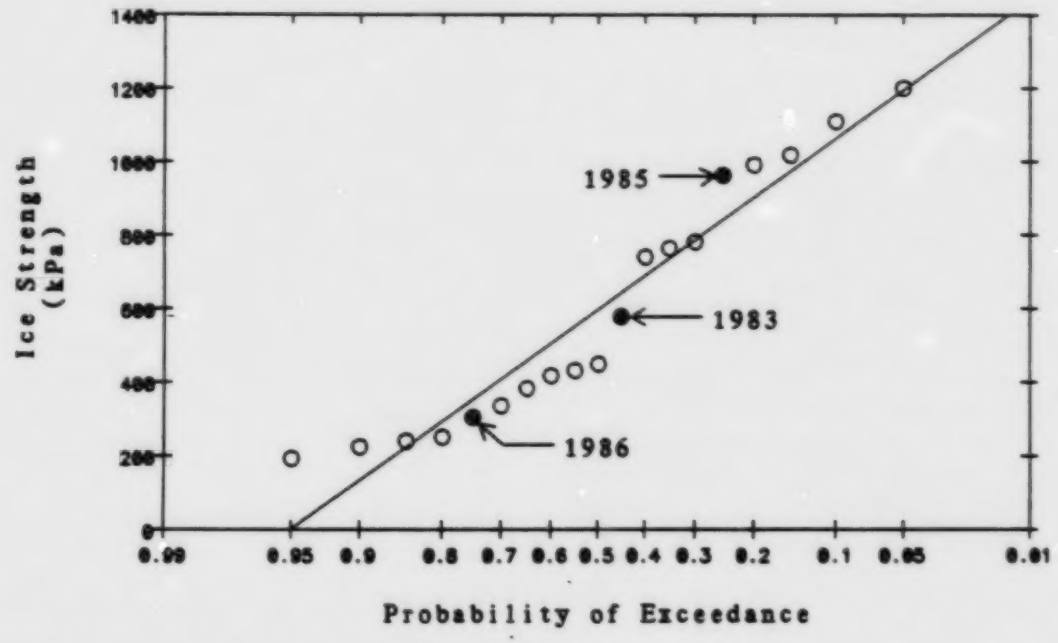

Figure 8 Compressive ice strength frequency distribution

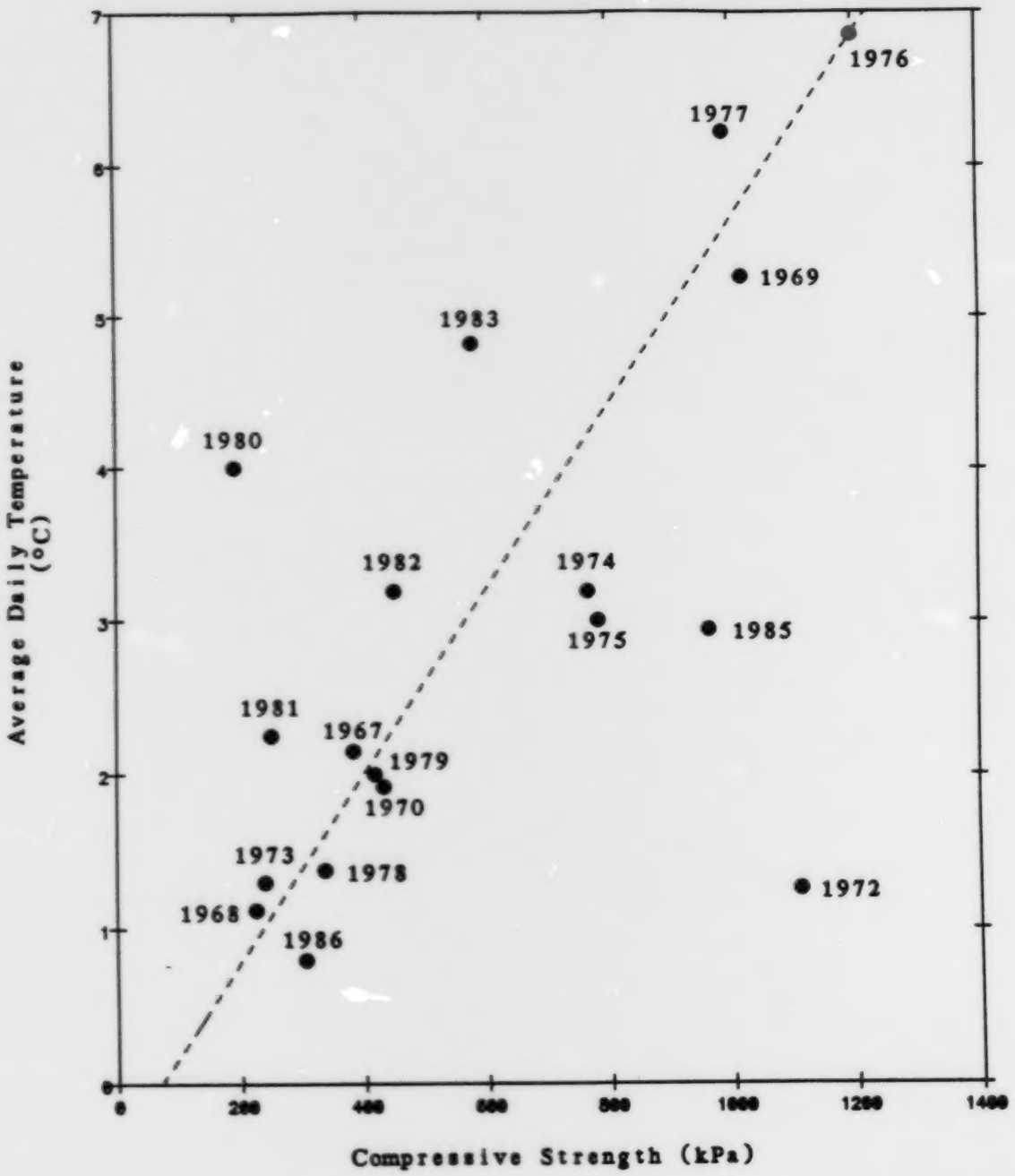

Figure 9 Comparison of the meteorological index with the compressive strength of ice at breakup

The use of a more complex index would likely reduce the scatter in this data. The index should include measures of snowcover, winter ice thickness and radiation input in conjunction with pre-breakup temperature data (Andres, 1988). If there is enough snowcover to produce a significantly rapid rise in water level when it melts, the ice cover will lift and crack, causing breakup to occur earlier than if less snow had been available for runoff. The maximum winter ice thickness is needed as a measure of the winter severity. During a severe winter, a thick ice cover may be produced which would take a long time to melt; while, during a mild winter, a thin ice cover may form which would deteriorate quickly. Radiation input should also be taken into account because it contributes significantly to the deterioration of the ice cover. If all these variables are taken into account, a more accurate index could be developed to predict the severity of breakup.

5.0 Summary and Recommendations

The ice runs of 1983, 1985, and 1986 were not extreme events. The 1983 ice run produced a maximum ice force of 0.52 MN when an ice floe with an estimated strength of 580 kPa failed by crushing. No ice forces were measured in 1984. In 1985, an estimated strength of 960 kPa was obtained from a maximum crushing force of 0.85 MN. In 1986, a bending failure produced a maximum ice force greater than 0.43 MN and an estimated strength of at least 300 kPa. A 1-in-100 year ice strength of approximately 1500 kPa was estimated using a simple frequency analysis although the largest strength observed for major floes was less than 1200 kPa. A range of site conditions should be studied to determine how ice forces and ice strengths vary with location and environment.

In both 1985 and 1986, the ice strengths at breakup were considerably lower than the ice strengths obtained from insitu tests done about a month before breakup. The average positive daily mean temperature prior to breakup is not an adequate index to predict the maximum ice strength at breakup. A better meteorological index which includes factors such as snowmelt, winter ice thickness, and radiation input should be developed to estimate ice strengths without direct measurement.

There are several distinct ice failure modes: crushing, bending and splitting failure modes as well as impact events which product ice forces on bridge piers. The relationship between ice forces and ice strengths and thicknesses is determined by the failure type. Crushing forces vary directly with ice thicknesses, while bending forces vary with the square of ice thicknesses. Crushing forces may be limited by the size of the floe impacting on the pier. If the size of the ice floes are limited by river geometry, a reduction factor may be applicable. The different types of analysis required for various ice failure modes should be addressed in bridge design codes.

6.0 References

Afanas'ev, V.P., Dolgopolov, Y.V. and Shvaishstein, Z.I., 1971. "Ice pressure on individual marine structures", in Ice Physics and Ice Engineering, ed. G.N. Takolev, Leningrad, U.S.S.R.. Translated by Israel Program for Scientific Translations, Jerusalem, Israel.

Alberta Environment, 1983. Water Supply Outlook and Snow Survey Bulletin. May edition. Prepared by the Alberta River Forecast Centre and the Survey Branch, Edmonton, Alberta.

Alberta Environment, 1984. Water Supply Outlook and Snow Survey Bulletin. May edition. Prepared by the Alberta River Forecast Centre and the Survey Branch, Edmonton, Alberta.

Alberta Environment, 1985. Water Supply Review and Snow Survey Summary. April edition. Prepared by the Alberta River Forecast Centre and the Survey Branch, Edmonton, Alberta.

Alberta Environment, 1986. Water Supply Review and Snow Survey Summary, 1985/1986. Prepared by the Alberta River Forecast Centre and the Survey Branch, Edmonton, Alberta.

Andres, D.D., 1988. Observation and prediction of the 1986 breakup on the Athabasca River upstream of Fort McMurray, Alberta. Alberta Research Council. Resource Technologies Department, Report No. SWE-88/03.

Canadian Standards Association 1978. Design of Highway Bridges. Standard CAN3-S6-M78, pp. 34-36.

Frederking, R.M.W. 1980. Dynamic ice forces on an inclined structure. Proceedings IUTAM Symposium on the Physics and Mechanics of Ice, Denmark, ed. P. Tryde, pp. 104-116.

Gerard, R. 1978. Mode of failure and the analysis of ice loads on bridge piers. Proceedings 4th Symposium on Ice Problems, International Association for Hydraulic Research, Lulea, Sweden, pp. 335-348.

Huiskamp, W.J. 1983. Ice force measurements on bridge piers 1980-1982. Alberta Research Council, Civil Engineering Department, Report no. SWE 83-1.

Korzhavin, K.N. 1962. Action of ice on engineering structures. U.S.S.R. Academy of Science, Siberian Branch, Draft Translation 260 Cold Regions Research and Engineering Laboratory.

Lipsett, A.w. and Gerard, R. 1980. Field measurements of ice forces on bridge piers 1973-1979. Alberta Research Council, Transportation and Surface Water Engineering Department, Report No. SWE 80-3.

Michel, B. 1978. Ice Mechanics. Les Presses de L'universite Laval.

Neill, C.R. 1970. Ice pressure on bridge piers in Alberta, Canada. International Association for Hydraulic Research, Proceedings 1st International Symposium, Reykjavik, Iceland, pp. 6.1.1-6.1.8.

Neill, C.R. 1976. Dynamic ice forces on piers and piles. An assessment of design guidelines in the light of recent research. Canadian Journal of Civil Engineering, vol. 3, pp. 305-341.

Neill, C.R., Saunders, H.D. and Schultz, H., 1971. Measurements of ice forces on bridge piers, 1970 and 1971. Alberta Cooperative Research Program, Internal Report No. REH 71/1.

Neill, C.R. and Schultz, H. 1973. measurements of ice forces and strengths, spring 1972. alberta coopertive research program, internal report no. REH 73/1.

Roads and Transportation Association of Canada 1980. Ice effects on bridges. ed. C.R. Neill, Roads and Transportation Association of Canada, 123 p.